



## The geometry of volcano flank terraces on Mars

Paul K. Byrne<sup>a,b,\*</sup>, Benjamin van Wyk de Vries<sup>b</sup>, John B. Murray<sup>c</sup>, Valentin R. Troll<sup>d,a</sup>

<sup>a</sup> Department of Geology, Trinity College Dublin, Dublin 2, Ireland

<sup>b</sup> Laboratoire Magmas et Volcans, Université Blaise-Pascal, 63038 Clermont-Ferrand, France

<sup>c</sup> Department of Earth Sciences, The Open University, Milton Keynes MK7 6AA, United Kingdom

<sup>d</sup> Department of Earth Sciences, Uppsala University, 752 36 Uppsala, Sweden

### ARTICLE INFO

#### Article history:

Received 4 August 2008

Received in revised form 8 January 2009

Accepted 15 January 2009

Available online 19 March 2009

Editor: T. Spohn

#### Keywords:

volcano  
flank  
terrace  
volcanotectonic  
Mars  
Earth

### ABSTRACT

Flank terraces are subtle, expansive structures on the slopes of many large Martian shield volcanoes. Several terrace formation hypotheses – including self-loading, lithospheric flexure, magma chamber tumescence, volcano spreading, and shallow gravitational slumping – have been suggested. Terraces are not readily visible on photogeological data; consequently, terrace geometry has not yet been comprehensively described. Terrace provenance, therefore, is poorly understood. We used three-dimensional Mars Orbiter Laser Altimeter (MOLA) data to characterise the geometry of these elusive structures, with a view to understanding better the role that flank terraces play in the tectonic evolution of volcanoes on Mars. Terraces have a broad, convex-upward profile in section, and a systematic “fish scale” imbricate stacking pattern in plan. They are visible at all elevations, on at least nine disparate Martian volcanoes. Terrace-like features also occur on three shield volcanoes on Earth, an observation not recorded before. Analysis of a suite of morphometric parameters for flank terraces showed that they are scale-invariant, with similar proportions to thrust faults on Earth. We compared predicted formation geometries to our terrace observations, and found that only lithospheric flexure can fully account for the morphology, distribution, and timing of terraces. As a volcano flexes into the lithosphere beneath it, its upper surface will experience a net reduction in area, resulting in the formation of outward verging thrusts. We conclude, therefore, that flank terraces are fundamental volcanotectonic structures, that they are the surface expressions of thrust faults, probably formed by lithospheric flexure, and that they are not restricted to Mars.

© 2009 Elsevier B.V. All rights reserved.

### 1. Introduction

Flank terraces are topographically subtle, laterally extensive bulge-like structures that occur on the slopes of a number of large Martian shield volcanoes. They were first observed on Mariner 9 images, and later on Viking data. Several prior studies have addressed these structures, yet there is no consensus as to their morphology, distribution, or origin. We provide a thorough description of their morphology and distribution, necessary for any complete explanation of their origin within the context of the tectonic and constructional evolution of the volcanoes on which they occur.

#### 1.1. Flank terrace observations

Terraces were first noted by Carr et al. (1977) on the upper flanks of Olympus Mons (Fig. 1a), and were later described more quantitatively by Morris (1981). Terraces were then reported on the flanks of

Arsia, Pavonis, and Ascraeus Montes (Thomas et al., 1990) (Fig. 1b, c, d). Early works presented sketch maps of terraces on Olympus Mons, drawn from Viking orbiter data, and showed terraces as characterised by long, sinuous traces (Fig. 2a, b). Other features on these volcanoes have been described through comparison with similar structures on Earth (Wilson and Head, 1994; Bleacher et al., 2007), yet no structure analogous to flank terraces has so far been recognised.

#### 1.2. Proposed formation mechanisms

Whilst Carr et al. (1977) included terraces in an overview of salient tectonic structures on Olympus Mons, they did not propose an origin for these flank structures. Morris (1981) interpreted terraces on Olympus Mons as having formed from high-angle reverse faults, in response to subsidence of the edifice into its central vent or magma chamber. Thomas et al. (1990) related the convex terrace profile to an origin due to thrust faulting. Using a finite element model for elastic stresses, they concluded that volcano self-loading – the effect of a volcano's mass upon its own strata – generates compressive flank stresses that exceed the yield strength of basalt, leading to radial thrusting. McGovern and Solomon (1993) also regarded flank terraces as compressional structures. Again using finite element models, they

\* Corresponding author. Department of Geology, Trinity College Dublin, Dublin 2, Ireland. Tel.: +353 1 896 1244.

E-mail addresses: [byrnepk@tcd.ie](mailto:byrnepk@tcd.ie) (P.K. Byrne), [b.vanwyk@opgc.univ-bpclermont.fr](mailto:b.vanwyk@opgc.univ-bpclermont.fr) (B. van Wyk de Vries), [j.b.murray@open.ac.uk](mailto:j.b.murray@open.ac.uk) (J.B. Murray), [valentin.troll@geo.uu.se](mailto:valentin.troll@geo.uu.se) (V.R. Troll).

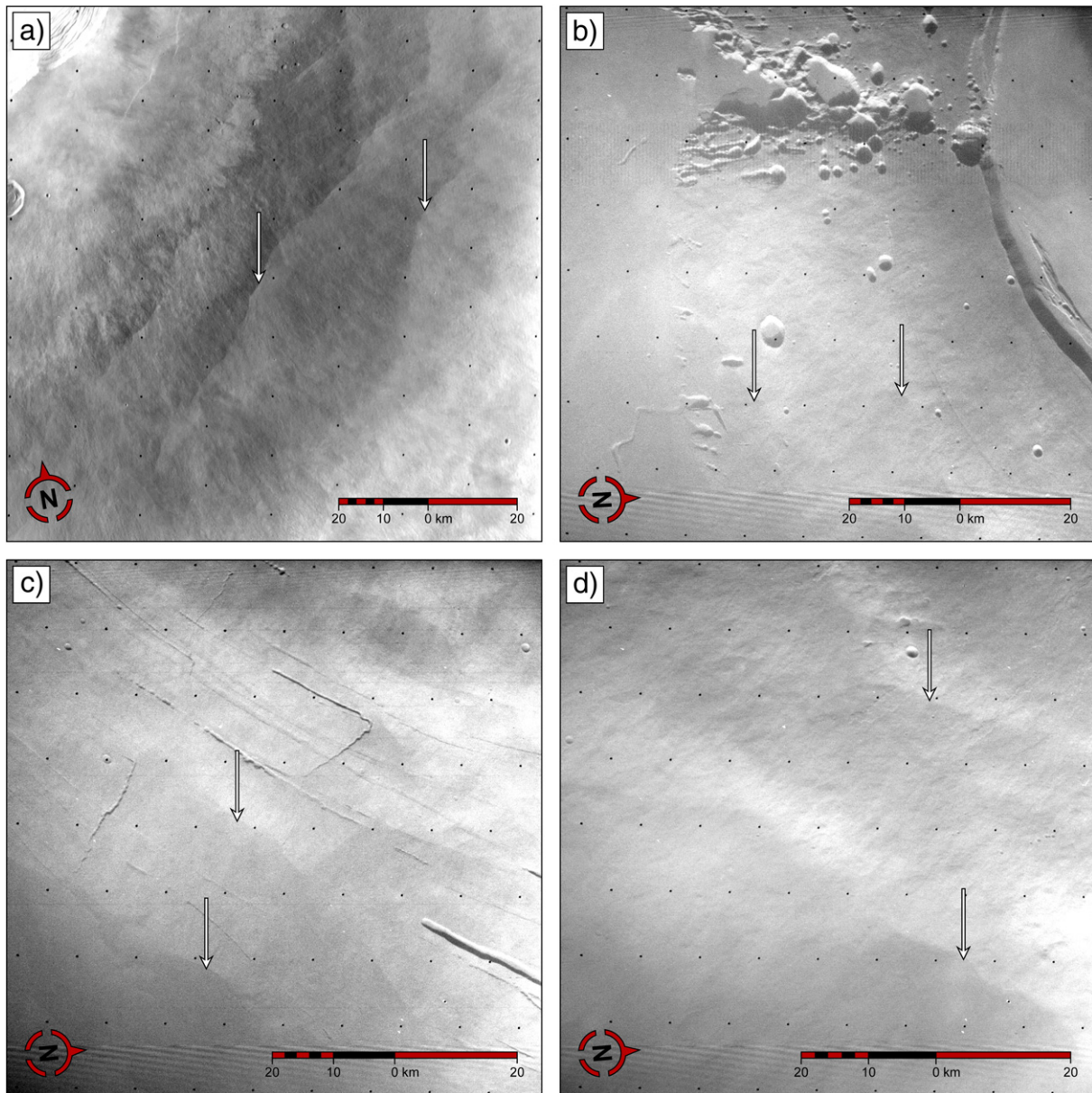


**Fig. 1.** Excerpts of Viking orbiter data used in previous terrace studies (i.e. Carr et al., 1977; Thomas et al., 1990). Readily visible terrace traces are highlighted (heads of white arrows). The moderate resolution and suboptimal lighting conditions of these data hide the extent and complexity of terrace geometries. a.) The SE flank of Olympus Mons (frame 046B32); b.) the S flank of Arsia Mons (frame 210A45); c.) the SE flank of Pavonis Mons (frame 210A37); and d.) the SE flank of Ascraeus Mons (frame 210A15).

assessed the contribution of lithospheric flexure to edifice stresses, and how flexure affects strain geometries. Investigating both incremental and instantaneous edifice construction, their models predicted that where a volcano was welded to a flexing lithosphere, early lava units would undergo thrusting due to compression. Later units were not affected, however, and non-welded volcanoes experienced no radial flank thrusting at all. As their forecasts for other tectonic structures (e.g. concentric graben) better correlated to basally detached edifices, McGovern and Solomon (1993) ultimately favoured a non-welded model of volcano development, in contrast to that required for flank thrusting. Citing the simple physical models of Marti et al. (1994), Crumpler et al. (1996) argued that magma chamber growth might steepen the upper flanks of a volcano, through uplift of overlying material along inward-dipping thrusts. These workers suggested that terraces might therefore be folds over blind thrust faults that accommodate magma chamber inflation.

In contrast to previous studies, Cipa et al. (1996) preferred an extensional origin for flank terraces, suggesting they were bounded by

outward-dipping normal faults. Montési (1999, 2000) acknowledged that terraces might be either compressional or extensional in origin, but regarded flank terraces and concentric graben on the Tharsis Montes as mutually exclusive structures. Discounting gravitational spreading as a formation mechanism for the graben, Montési (2000) instead proposed that flank stress relaxation led to terrace formation, agreeing with the extensional origin proposed by Cipa et al. (1996). Finally, in a recent study of gravitational deformation within volcanoes, Morgan and McGovern (2005) suggested that, as folds over low-angle thrusts, terraces might represent the toes of shallow gravitational slumps that formed in response to volcano spreading.

### 1.3. Rationale for this study

Most previous work on terraces has been based on remotely sensed photogeological images alone. Due to their low relief and large spatial extent, however, flank terraces are not easily visible in images without optimal lighting geometries (Thomas et al., 1990). Terrace

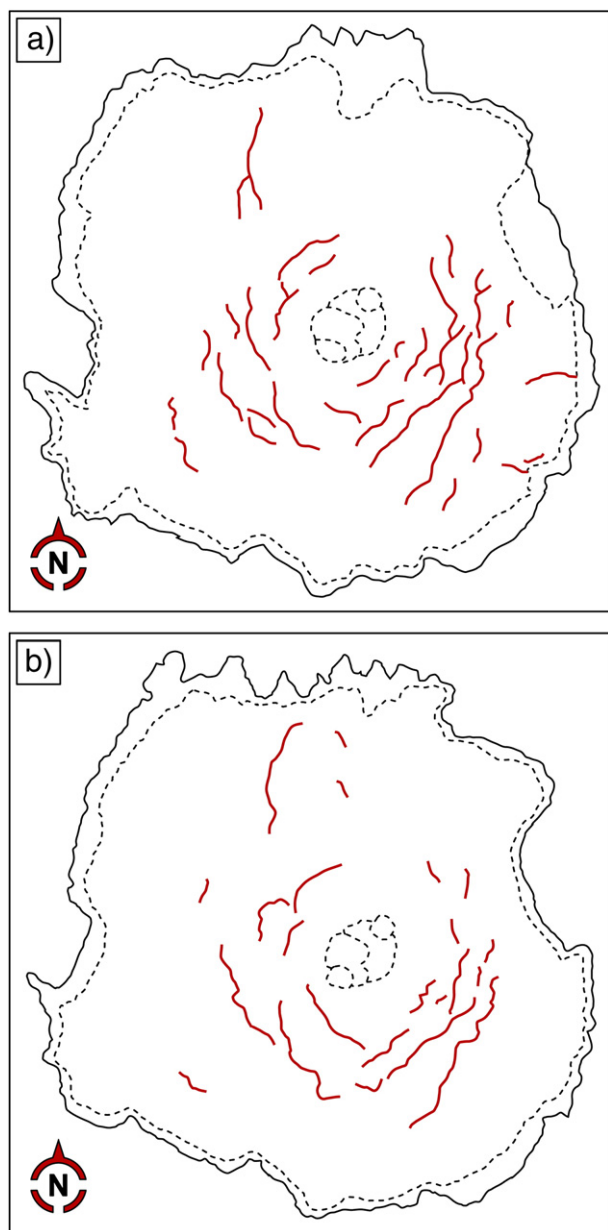


**Fig. 2.** Sketch maps of terrace traces on Olympus Mons, derived from photogeological data, after a.) Fig. 2 of Morris (1981) and b.) Fig. 2 of Thomas et al. (1990). The base of the volcano is marked with a solid light line. The top of the basal scarp, and the caldera complex, are marked with dashed lines. The sinuous terrace traces identified by these authors are indicated with heavier lines.

geometry, as a function of morphology and distribution, cannot therefore be fully determined from images alone, and so remains to be quantified. Such lighting considerations do not affect Digital Terrain Model (DTM) data, which are therefore eminently suitable for use in terrace mapping and analysis, and which provide a superior data set with which to study flank terrace geometry and origin.

In this paper, we aim to describe Martian flank terrace morphology and distribution comprehensively using DTM data. We characterise the geometry of these structures on recognised terraced volcanoes: Olympus, Ascraeus, Pavonis, and Arsia Montes (e.g. Thomas et al., 1990; McGovern and Solomon, 1993), Elysium Mons (Byrne et al., 2007) and Hecates Tholus (Byrne et al., 2007; Plescia, 2007); as well as three other shields not previously reported as terraced: Alba Patera, Albor Tholus, and Uranus Patera. We also present evidence for terracing on three volcanoes on Earth, where flank terraces have not been reported before: Etna (Sicily), Mauna Loa (Hawaii), and

Tendürek Dagi (Turkey). As the geometry of tectonic structures is primarily a function of formation, we appraise the validity of existing formation hypotheses by comparing predicted structural geometries with those observed on Mars, with a view to understanding the role of terraces within the tectonic evolution of Martian shield volcanoes.

#### 1.4. Volcanoes studied

Of the 22 large volcanic edifices on Mars (Crumpler et al., 1996; Plescia, 2004), nine volcanoes appear terraced, and are the focus of this study. Key morphometric data for these volcanoes are given in Table 1. Zimbleman and Edgett (1992) describe the morphologies and associated landforms of the Tharsis Montes in detail, whilst Mouginitis-Mark et al. (1984) review the geology of the Elysium Planitia volcanoes. For an overview of all significant volcanic landforms on Mars, the reader is directed to Hodges and Moore (1994) and Plescia (2004).

#### 1.5. Nomenclature used in this study

The terms “flank terrace” and “terrace” are used synonymously throughout this work to refer to the convex structures under discussion. It should be understood, however, that we regard “volcano flank terrace” as the full and correct term for these structures, so as to differentiate them from other geomorphological features that are also referred to as terraces – specifically caldera terraces (Roche et al., 2001) and fluvial terraces (Krall et al., 2008) – but which bear no other relation to the flank structures considered here. Additionally, we prefer the adjective “Terran” to “terrestrial” when describing volcanoes on Earth. Flank terraces may occur on edifices located on other rocky, differentiated planets beyond Earth and Mars (e.g. Venus, Mercury) to which the term “terrestrial” has been applied (Head and Solomon, 1981), but do not form the focus of this study.

## 2. Methodology

We derived products from three-dimensional DTM data and examined them within a Geographical Information System (GIS). We defined the representative terrace pattern from these data, and identified individual terraces. Measurements of certain terrace parameters were then taken and analysed.

### 2.1. DTM dataset

We used the publicly available USGS 128 pixel-per-degree equatorial Mars Orbiter Laser Altimeter (MOLA) gridded dataset, collected by the Mars Global Surveyor spacecraft during its primary mission phase (Zuber et al., 1992; Smith et al., 2001). The dataset has topographic coverage of Mars between 88° N and 88° S, and has an innate equidistant cylindrical projection; ground resolution is approximately 460 m.

### 2.2. Data preparation

Each study volcano was extracted from the MOLA dataset using ESRI ArcMap 9.1, and displayed with a sinusoidal, orthographic projection. The Spatial Analyst extension in ArcMap was then used to generate slope maps of each edifice. A slope map is the product of calculating the rate of maximum change in elevation from each cell in a surface, and is therefore useful for identifying subtle features, or determining regional slopes. All slope maps were assigned the same colour stretch; steeper slopes have darker colours. In each case, slopes were automatically classified into fifteen bins. This number of divisions was chosen to ensure both large scale and subtle trends in slope were visible, to enable detection of as many terraces as possible.

**Table 1**  
Morphometric data for the nine Martian volcanoes studied.

Volcano	Edifice size (km)	Base elevation (m)	Summit elevation (m)	Relief (m)	Volume (m <sup>3</sup> )	Flank slope (°)	Latitude	Longitude
Alba Patera	1015 × 1150	1049	6849	5800	1.8 × 10 <sup>15</sup>	1.0	40.6	−110.0
Albor Tholus	157 × 164	−269	3931	4200	2.9 × 10 <sup>13</sup>	5.0	19.0	150.2
Arsia Mons	461 × 326	6076	17776	11700	9.2 × 10 <sup>14</sup>	5.0	−9.5	−120.5
Ascraeus Mons	375 × 870	3350	18250	14900	1.1 × 10 <sup>15</sup>	7.0	11.1	−104.2
Elysium Mons	375 × 375	1513	14113	12600	2.0 × 10 <sup>14</sup>	7.0	24.5	146.7
Hecates Tholus	177 × 187	−1746	4854	6600	6.7 × 10 <sup>13</sup>	6.0	31.5	150.0
Olympus Mons	840 × 640	−610	21290	21900	2.4 × 10 <sup>15</sup>	5.0	18.3	−133.2
Pavonis Mons	380 × 535	5664	14064	8400	3.9 × 10 <sup>14</sup>	4.0	1.1	−122.6
Uranius Patera	242 × 280	1955	4955	3000	3.5 × 10 <sup>13</sup>	3.0	26.5	−92.8

Values for edifice size, relief, volume, and flank slope are from Plescia (2004). Volumes and sizes are calculated with respect to a reference surface for each volcano, which is typically the topographically lower change in slope of that edifice. Summit elevation values are taken from the MOLA dataset (Smith et al., 2001), and are relative to the IAU2000 definition for Mars. Base elevations are then calculated from the relief values of Plescia (2004). Latitude and longitude values are adapted from Crumpler et al. (1996), and are given here relative to a coordinate system with a centre of longitude of 0°.

### 2.3. Terrace definition

Thomas et al. (1990) described terraces on Olympus Mons as having a sharp break in slope at their base, and gentle convex topographic profiles. On a slope map of Olympus, a terrace thus appears as a generally planar area bounded by steeper slopes further from the volcano centre, that then terminate against lower, flat terrain (Fig. 3). We used this definition as the basis for identifying flank terraces on this and other edifices. By then marking the boundary between steeper slopes and the following flatter terrain, we delineated individual terrace traces.

### 2.4. Morphometric measurements

To characterise flank terraces as quantitatively as possible, and to allow meaningful comparison between volcanoes, we measured a set of parameters from each terrace sketch map that describes both terrace morphology (the lengths and gradient), and distribution (in terms of elevation and position) (Fig. 4a, b). ArcMap's Editor functions were used to manually delineate terraces, and obtain these para-

meters from the sketch maps. We only included a terrace boundary where it was clear; structures that resemble terraces but remain equivocal at the resolutions of our datasets were ignored. All discrete bounding traces were then counted for every edifice, giving the total number of terraces for each volcano.

#### 2.4.1. Morphology

Measurements of terrace traces provided a bounding length value for each terrace (Fig. 4a: 1), whilst a circumferential length value was obtained by measuring the straight-line distance between the ends of a terrace boundary (Fig. 4a: 2). Values for radial length (Fig. 4a: 3) and vertical height (Fig. 4a: 4) were calculated from the horizontal and vertical differences, respectively, between the midpoints of a terrace bounding edge and the line joining its ends. The slope of a line joining these two points served as the gradient value for a terrace (Fig. 4a: 5), and was compared with those of other terraces, and with that of the flank upon which it sits. Average terrace lengths and gradients for each shield were also calculated.

#### 2.4.2. Distribution

A single terrace may occupy a range of elevations. A specific elevation value was therefore attained for each terrace by measuring the elevation at the midpoint of its bounding edge (Fig. 4a: 6). The range of elevations at which terraces occur on each volcano was then plotted as a percentage of edifice height (Fig. 4b).

## 3. Flank terrace observations

### 3.1. Visibility

Flank terraces remain detectable on slope maps, despite their subtle topography, irrespective of the ages of the Martian shields upon which they occur (cf. Neukum et al., 2004). Some late-stage volcanism has obscured or tempered terrace traces in places, indicating that terrace development was, at least in part, contemporaneous with flank volcanism (Thomas et al., 1990). The general terrace morphology is still present, however, even where partly covered by late lava flows.

### 3.2. Morphology

MOLA transects across Olympus Mons confirm that the terrace profile is characterised by a broad, convex-upward form, with a near-flat upper surface whose slope increases towards the terrace base, as reported by Thomas et al. (1990) (Fig. 5). DTM-derived slope maps provide a clear insight into terrace plan view morphology, and show that terrace bases are delineated by convex-outward arcuate traces, and are generally not laterally continuous. Terraces are configured in an overlapping manner, wherein the upper portion of one terrace is

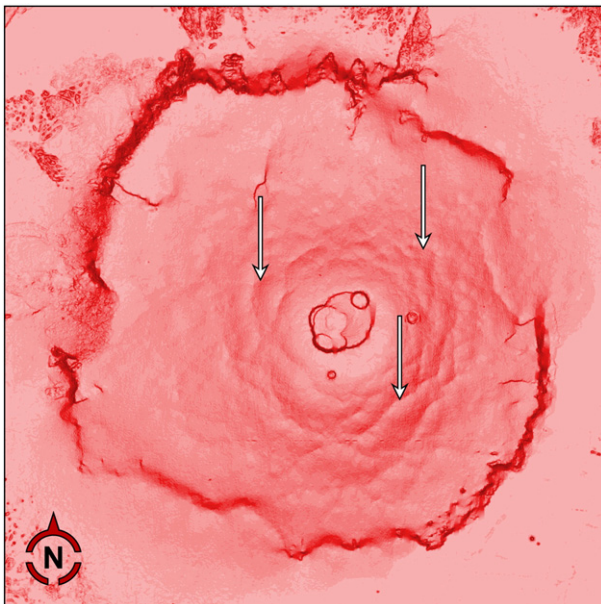


**Fig. 3.** MOLA-derived slope map of Olympus Mons. Slopes are classified into fifteen bins, and colours darken with increasing gradients. The steep basal scarp thus appears dark, whilst the summit plateau is light coloured. The pattern of arcuate areas of darker colour juxtaposed against zones of lighter colour denotes the flank terraces upon Olympus (examples at head of white arrows).

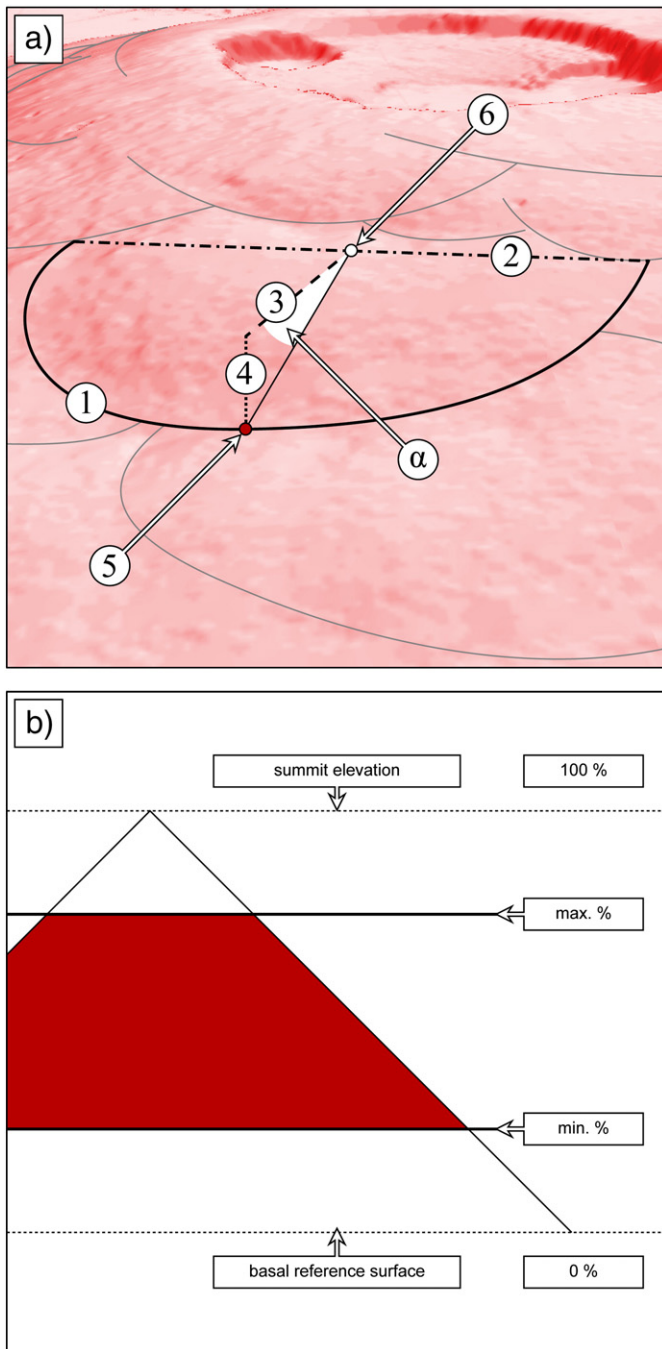


**Fig. 4.** Schematic diagrams showing the various parameters we measured from the terrace traces. a.) The parameters describing terrace morphology: (1) bounding edge length (solid line); (2) chord length (dot-dashed line); (3) radial length (dashed line); and (4) vertical height (dotted line). Shown too are the bounding line and chord line midpoints (5 and 6, respectively), from which slope and elevation values were obtained, and ( $\alpha$ ), the angle which describes the terrace gradient. b.) Terrace elevation as a percentage of volcano height, calculated with respect to the basal reference surface of each volcano, derived from the relief values of Plescia (2004). The shaded area on the volcano represents the elevation range in which terraces occur. Note that in some cases, the reference surface may lie above some terraces, resulting in negative percentage values for elevation range minima (Table 2).

superposed upon a topographically lower, adjoining terrace. This imbricate arrangement forms a distinctive “fish scale” stacking pattern in plan (see the terrace sketch maps for each volcano in Figs. 6 and 7). Where terraces occur close together, many bounding traces terminate at the midpoint of a topographically higher terrace.

### 3.3. Distribution

Whilst the “fish scale”-stacking pattern is systematically manifest upon every terraced volcano, the number, size, location, and consequently plan view distributions of terraces on each shield vary considerably. MOLA slope map-derived terrace sketch maps are provided here for all volcanoes in our study, which includes nine shields on Mars, and three on Earth (the Terran edifices are discussed separately in Section 4.5). Slope maps and terrace distribution plots for each volcano are also presented. Alba Patera, Albor Tholus, Arsia Mons, Ascraeus Mons, Elysium Mons, and Hecates Tholus are shown in Fig. 6, whilst Olympus Mons, Pavonis Mons, and Uranius Patera, as well as the three Terran shields (Etna, Mauna Loa, and Tendürek Dagi), are shown in Fig. 7. Larger versions of these figures are provided as Supplementary material.

### 3.4. Morphometric data

The key geometrical parameters described in Section 2.4 were measured for each terrace in the study dataset (1613 in total), and are discussed in Sections 4.2 and 4.3. Average values for Mars and Earth are presented in Table 2. The entire dataset for each volcano is provided as Supplementary material.

## 4. Discussion

### 4.1. Timing

That terraces are still evident today suggests either they are late-stage structures, or they form continually. They may reflect a single phase of deformation, or the latest increment of strain in an ongoing process. If the former applies, terraces develop upon some of the last units to be emplaced, towards the end of the main shield-building phase. If terraces are recurring structures, their bounding faults may serve to accommodate shape change in a volcano throughout its lifetime.

### 4.2. Morphology

Normal faults tend to manifest as abrupt changes in slope, and where accommodating extension on a volcano, occur as concave-outward structures in plan (van Wyk de Vries and Borgia, 1996). Thrusts are characterised by lobate leading edges, often with a convex-outward plan configuration (Twiss and Moores, 1992, p. 96–112). The convex-upward terrace profile is thus consistent with thrust fault morphology in a compressive stress regime, and is unlike that produced by normal faulting due to extension. The upper flat area of a terrace probably corresponds to the culmination of a thrust anticline, and may be further flattened by sediment accumulation (Borgia and van Wyk de Vries, 2003). Terrace traces often terminate close to the midpoints of adjoining terraces, possibly due to geometric coherence (Walsh and Watterson, 1991), whereby strain is accommodated across several structures in a single fault system. This relationship between terrace traces, and the “fish scale” pattern in general, is suggestive of a systematic method of flank terrace formation. Moreover, as the same “fish scale” pattern appears on each terraced volcano, the mechanism of terrace formation must also be similar for every such shield. Key terrace morphology parameters for both Mars and Earth are discussed below (Fig. 8).

#### 4.2.1. Displacement

Maximum displacement along a thrust fault usually occurs normal to the midpoint of a chord joining its ends (the bow-and-arrow rule). A log–log plot of strike length versus maximum horizontal displacement for thrusts on Earth yields a linear relationship (Elliott, 1976). As the displacement of a thrust fault is proportional to the amplitude of

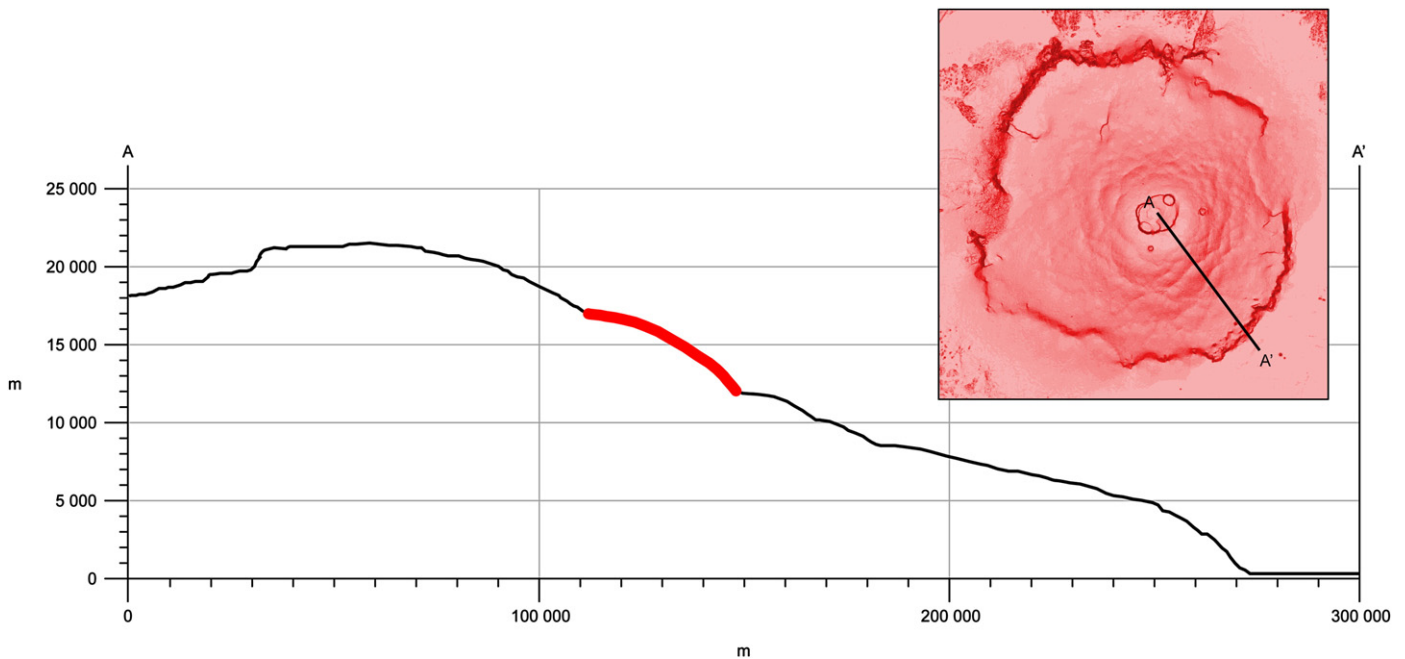


**Fig. 5.** The characteristic cross-sectional terrace morphology derived from DTM data. A  $5\times$  vertical exaggeration cross-section taken across the SE flank of Olympus Mons shows the convex-upward terrace profile; a single terrace is highlighted (heavy line). The location of the transect is shown on a slope map of the volcano (inset, top right). This convex-upward profile is consistent with thrust fault morphology.

its surface expression (e.g. a fault propagation fold or fault scarp), we use terrace radial length as a rough proxy for fault displacement. When plotted against terrace chord (strike) length, then, our data also described a linear relationship (Fig. 8a). Terrain length values plot in the same fashion as Martian values. Our data follow a power law function, and are scale-invariant. That they behave similarly to data for known tectonic structures on Earth further supports the possibility that flank terraces are the surface expressions of thrust faults. If so, their low amplitude morphology represents shortening on the flanks of probably less than 10%. We suggest analogue modelling of terrace formation could help establish the relationship between terrace morphology and flank shortening.

#### 4.2.2. Shape

A linear plot of terrace bounding length versus circumferential, radial, and vertical length values indicates that terrace proportionality is also scale invariant: that is, the relative ratios of each of these parameters remain the same across all scales. Therefore, whilst terrace size may vary between volcanoes, and even across a single edifice, flank terrace shape as described by these parameters remains the same. This relationship applies equally for Mars and Earth (Fig. 8b). Terrace size may differ upon and between volcanoes due to a range of factors (see Section 4.3.2).

#### 4.2.3. Slope

The ease with which a terrace can be seen in images is a function of its slope – specifically, the gradient of its leading edge. Terrace formation may change the slope of the flank of the volcano on which it occurs. The average volcano slope may increase or decrease depending on the ratio of flat to steep areas on a terrace population, which in turn is contingent on the formation process. We suggest that the average volcano slope value (adopted from Plescia, 2004) is the most general and thus the best representative of volcanotectonic processes. Therefore, we take this general slope parameter for each volcano, and compare it with the average slope of all terraces for that volcano, to see if there is a general relationship. We observed a correlation between whole volcano flank slope and terrace slope values (Fig. 8c). Steeper, more prominent terraces occur on volcanoes with steeper

average flank values, e.g. Ascreaus Mons (Table 1). Terrace prominence is also greater on volcanoes with nested caldera complexes (e.g. Olympus and Ascreaus Montes). Terrace slopes may thus reflect the gradients of the flanks upon which they form. They might also be steepened if flank slopes increase, e.g. due to buttressing by regional topography (McGovern and Morgan, 2005). Alternatively, volcano flanks may be steepened by the reactivation of terrace bounding faults. There is currently insufficient evidence at this point, however, to explain the link between average terrace and average flank slopes, but here we simply report that there is a correlation.

### 4.3. Distribution

#### 4.3.1. Elevation

Flank terraces occur at all elevations on a volcano, and are not restricted to the upper flanks as previously reported (Thomas et al., 1990; McGovern and Solomon, 1993). For example, terraces on Olympus Mons extend from the summit to the top of the basal scarp; on Ascreaus Mons, they continue to the base of the volcano (Table 2). Therefore, as terraces are present across a range of flank elevations on all volcanoes studied, so too are the conditions responsible for terrace formation, whatever their nature.

#### 4.3.2. Plan view distribution

Some volcanoes display an axisymmetric distribution of terraces (e.g. Elysium Mons), whilst others show a high degree of asymmetric terracing (e.g. Uranus Patera) (see Figs. 6 and 7). Differences in internal architecture, volcano geometry, or regional-scale stresses could account for the variation in terrace distribution on the studied edifices, and for the range of terrace sizes observed.

### 4.4. Occurrence on Mars

Other factors can affect how and where terraces occur on Mars. Aeolian or mass-wasting processes might erode terrace traces, leaving some areas devoid of these structures, e.g. the NW flank of Arsia Mons. The erosional morphologies of the highland paterae (Crown and Greeley, 1993) are consistent with an absence of terraces on these

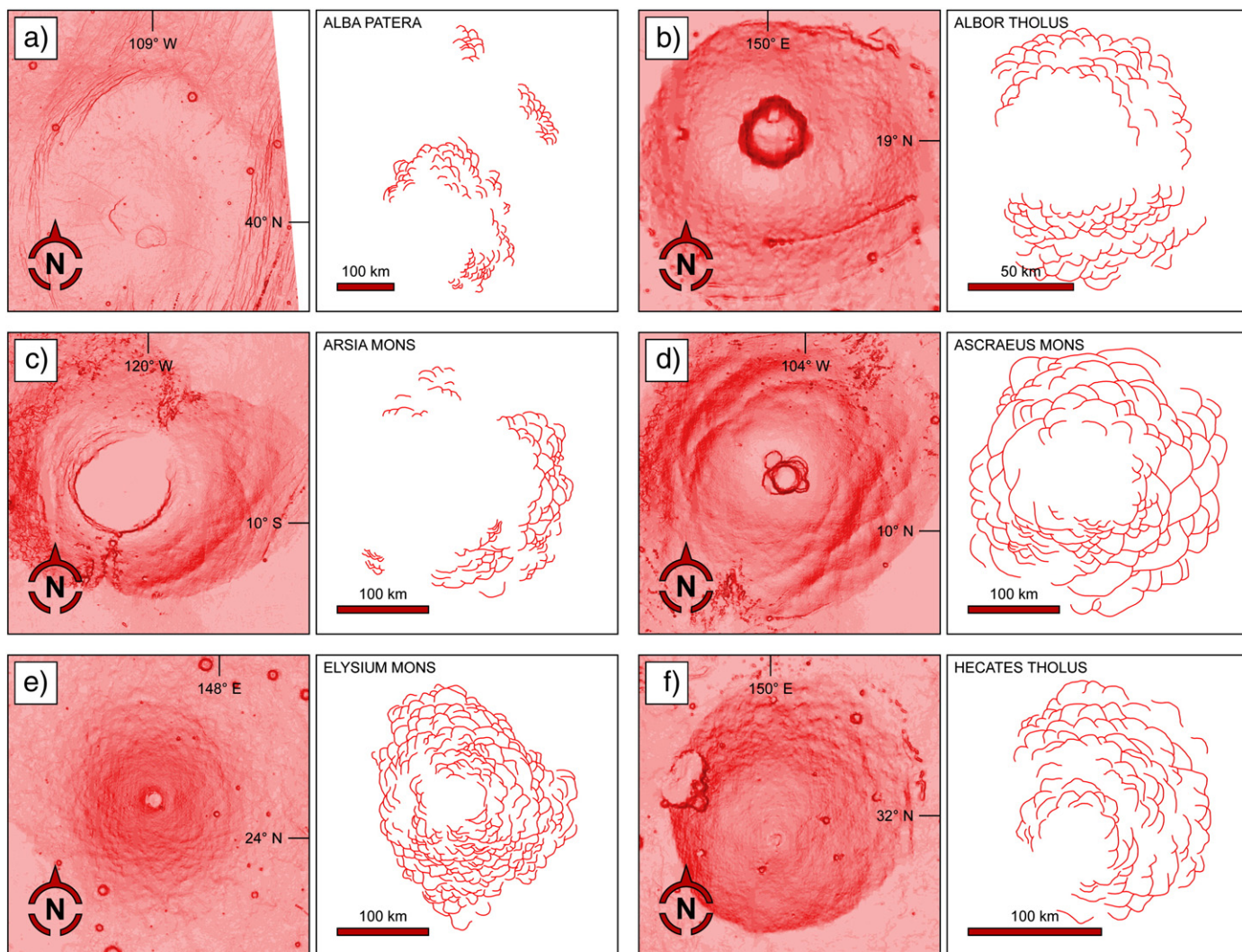


**Fig. 6.** The distribution of flank terraces on each shield studied. Volcanoes are displayed with their corresponding MOLA slope map (left of couplet), and derived terrace sketch map (right). Note the “fish scale” imbricate terrace pattern on each volcano (see Section 3.2). Latitude and longitude values are relative to a coordinate system with a centre of longitude of 0°. In this figure: a.) Alba Patera; b.) Albor Tholus; c.) Arsia Mons; d.) Ascraeus Mons; e.) Elysium Mons; and f.) Hecates Tholus.

volcanoes. DTM data quality also influences the location and number of terraces we report. MOLA interpolation artefacts occur on the W and E flanks of Albor Tholus, which in turn do not appear terraced. Additionally, terrace-like structures below MOLA resolution have been ignored. It is likely, therefore, that the total number of terraces on Mars presented herein is under-representative of the actual number. It is also likely that the total number of terraced volcanoes on Mars is greater than that which we provide here, and so should be treated as a minimum. Smaller shields such as Apollinaris Patera, Biblis Patera, Ceraunius Tholus, Jovis Tholus, Tharsis Tholus, Ulysses Patera, and Uranus Tholus could also be terraced, though high-resolution DTM data is required to test this.

#### 4.5. Occurrence on Earth

Similar considerations apply to Terran volcanoes. Vegetation, anthropological activity, increased rates of erosion and ongoing volcanism, the difficulty in seeing these structures in the field, and a lack of previous recognition of Terran flank terraces may preclude the identification of other terraced shields on Earth. However, thrust faults in the lava pile of the Palaeogene Mull volcano (Scotland) have produced anticlines and pop-up structures that may be analogous to flank terraces (Mathieu et al., *Bull. Volcanol.*, submitted), whilst

thrusting on the lower flanks of Concepción volcano (Nicaragua) might be the equivalent of terraces formed during the volcano’s early flexure and compressive phase (Borgia and van Wyk de Vries, 2003).

To investigate whether terrace-like structures occur elsewhere on Earth, we extended our study to include large shield volcanoes, using slope maps derived from the Shuttle Radar Topography Mission (SRTM) DTM dataset (Farr et al., 2007). This dataset has topographic coverage of Earth between 60° N and 54° S. We used SRTM data with a ground resolution of three arc-seconds (approximately 90 m). We introduce three shield volcanoes, Etna (Sicily), Mauna Loa (Hawaii), and Tendürek Dagi (Turkey), where structures resembling Martian flank terraces were also identified (Fig. 7d, e, f). These structures were mapped and measured according to the methods described in Sections 2.2, 2.3, and 2.4. Morphometric data for these structures are also given in Table 2.

All three Terran examples display terrace-like structures that do not have a clear volcano-constructional origin, yet have a convex-upward, convex-outward morphology and are distributed in a fish scale imbricate pattern, similar to flank terraces on Mars. These terrace structures are located in areas where flank-parallel compression may occur, but do not occur in areas where extension is dominant. They also correlate strongly with Martian terrace morphology (Fig. 8a, b). Thus, we propose that these features are possible

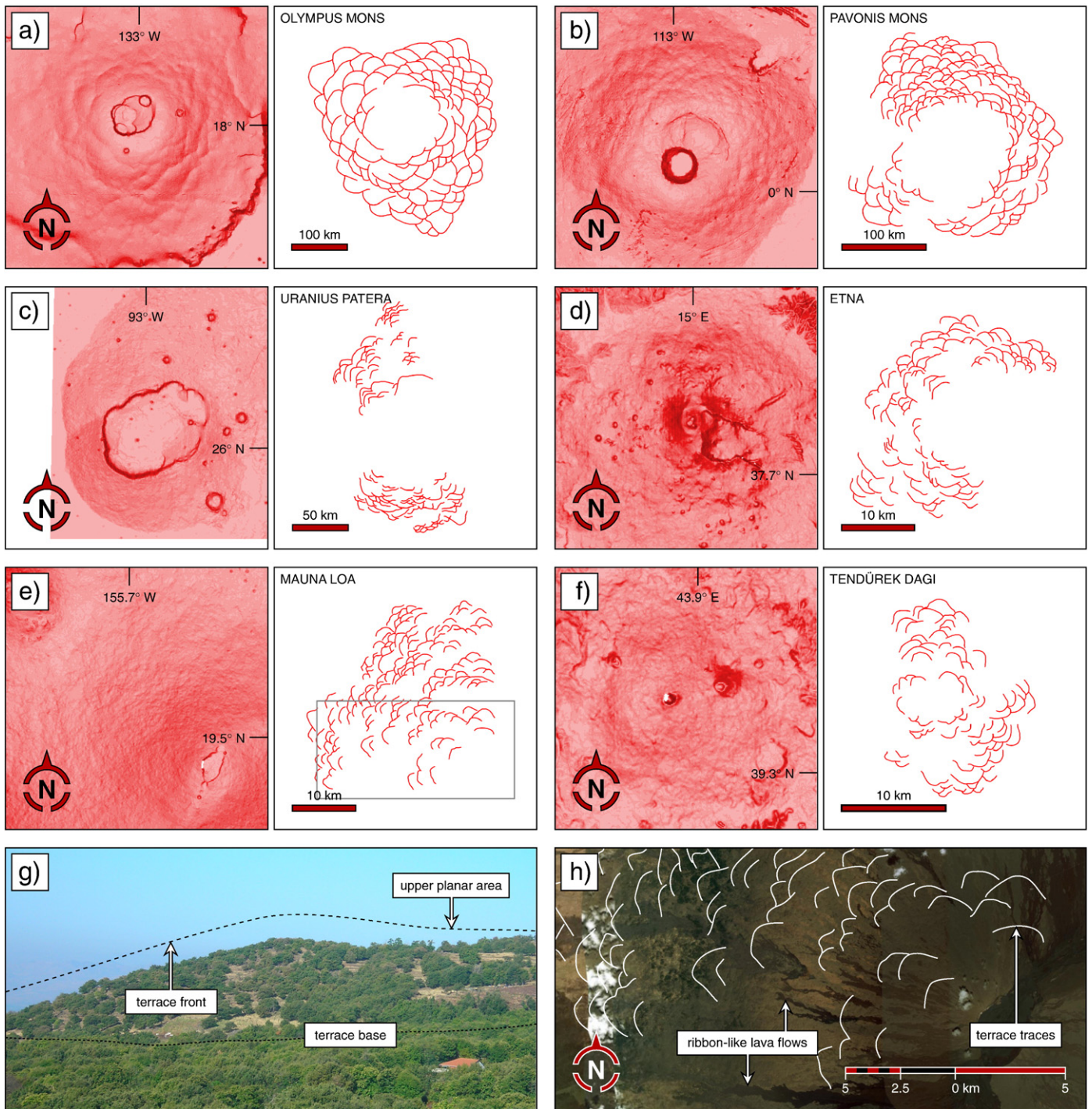


**Fig. 7.** As for Fig. 6, except in this figure: a.) Olympus Mons; b.) Pavonis Mons; c.) Uranius Patera; d.) Etna (Sicily); e.) Mauna Loa (Hawaii); and f.) Tendürek Dagı (Turkey). g.) Photograph of a terrace-like structure (labelled) on the SW flank of Etna. The structure is located at approximately 37.67° N, 14.92° E (WGS 84 map datum), and is ca. 1 km away; the image looks W. h.) Portion of satellite images taken from Google Earth™ (© 2008 DigitalGlobe), showing thin ribbon-like lava flows across the undulating surface of the NW flank of Mauna Loa. Both the flows and the terraces are labelled. Note the lack of spatial correlation between the terrace structures and the ribbon-like lavas. This image areal extent is outlined on the sketch map in e.).

Terran flank terraces, equivalent to those on Mars. Detailed mapping of fracture patterns on these volcanoes will be required to confirm terrace geometry and origin, but if confirmed as terraces, these structures may provide a valuable analogue for understanding volcanotectonic processes on Mars.

4.5.1. Etna

Mt. Etna volcano, Sicily, is a large lava shield with a central caldera-vent complex and N–S orientated main rift zones (Chester et al., 1985).

Spreading structures upon the E side of the volcano indicate that this flank is moving laterally eastwards into the Ionian Sea (Borgia et al., 1992). Etna is located in a N–S zone of regional contraction, and large-scale compressional features are observed at its southern foot (Branquet and van Wyk de Vries, 2001). Because of its large mass, its situation on ductile substrata, and because it is little eroded, Etna is a suitable site to explore for structures whose morphology matches that of flank terraces. On DTM-derived slope maps of Etna, we have observed arcuate, terrace-like features on the lower N and S flanks,

**Table 2**

Terrace morphometric data for nine Martian and three Terran volcanoes, acquired according to the methods described in Section 2.3 of the text.

Volcano	Number	Bounding length (km)	Circumferential length (km)	Radial length (km)	Vertical height (m)	Slope (°)	Elevation (m)		Elevation range (%)	
							Min.	Max.	Min.	Max.
<i>Mars</i>										
Alba Patera	127	27.0	21.6	6.3	128	1.2	931	5907	–2	84
Albor Tholus	122	11.9	9.4	2.8	258	5.5	–74	3381	5	87
Arsia Mons	115	20.0	16.3	4.6	459	5.7	8 289	16834	19	92
Ascraeus Mons	142	39.6	31.9	9.6	1084	6.2	3 874	17300	4	94
Elysium Mons	264	19.7	15.8	4.5	415	5.6	2 176	11362	5	78
Hecates Tholus	103	21.5	17.5	5.0	454	5.3	–3 561	3858	–28	85
Olympus Mons	118	51.2	38.7	13.4	1307	5.7	6378	20676	32	97
Pavonis Mons	167	26.2	20.8	6.2	487	4.5	6080	13457	5	93
Uranus Patera	121	12.8	10.8	2.6	115	2.7	1614	4071	–11	71
<i>Earth</i>										
Etna	107	2.3	1.8	0.5	83	9.6	625	1964	–11	44
Mauna Loa	150	2.3	1.9	0.5	55	6.0	1397	3685	–29	76
Tendürek Dagi	77	2.0	1.5	0.5	61	7.2	2388	3191	–61	53

The terrace number is the total number of unequivocal terrace structures mapped per volcano. Bounding, circumferential, and radial length values are rounded to the nearest hundred metres. Vertical height and elevation minima and maxima values are given to the nearest whole metre. Slope values to the first decimal point are presented. Elevation minima and maxima values for Mars are relative to the IAU2000 definition, and to the WGS 84 reference system for Earth. Elevation percentage ranges are calculated according to the relief values from Plescia (2004) (Fig. 4).

with a primary E–W distribution (Fig. 7d) and an average circumferential length of 1.8 km. These structures were visited in the field, but are extensively farmed and feature significant vegetation coverage (Fig. 7g). The convex-upward terrace shape is clearly visible, thus confirming our DTM observations, but any associated deformation proved impossible to identify conclusively on the ground. The lava flows are significantly autobrecciated and cut by many cooling fractures. For this reason we suggest that the strain during terrace formation would be accommodated by the movement of pre-existing fractures, and would thus be very difficult to detect at outcrop unless the strain amount were high. Strain localisation might develop some discrete structures, however. The thrust reported by Borgia et al. (1992) is located in our southern zone of likely terraces, and may in fact be the first reported field example of a terrace-forming thrust fault.

Geological maps of the volcano, our field inspection, and Google Earth™ images were also used to assess the relationship of the terrace-like structures with known eruptive features. The terraces are wider than any lava flow or eruptive structure (cones and aligned vents) on the volcano. In addition, eruptive constructs (e.g. cones, fissures, and lava flows) are aligned down-slope, whereas the terraces are arranged cross-slope. There is no clear spatial relationship between the terrace features and the observed constructional landforms, so whilst it is possible that the terraces have some obscure constructional origin from successive lava flows, they do not match any known eruptive morphology. They are distributed normal to the N–S direction of regional contraction, which has probably created the southern Catania anticline (Branquet and van Wyk de Vries, 2001). These terraces are absent from the spreading E flank of the volcano, but their position and orientation is consistent with a N–S tectonic shortening of Etna.

#### 4.5.2. Mauna Loa

The big island of Hawaii is dominated by the Mauna Loa and Kīlauea volcanoes. The surfaces of these volcanoes are not heavily eroded, and as there is known to be large-scale flexural sagging of the entire island, Hawaii is also a suitable candidate site for terraces. We observed an array of terrace-like features distributed over a wide area to the NW of the summit caldera on Mauna Loa (Fig. 7e). These features extend from near the summit to the base of the subaerial edifice, which abuts Hualālai and Mauna Kea. They have an average circumferential width of 1.9 km. DigitalGlobe images, visible via Google Earth™, reveals a 0.1-km scale undulating surface of long, ribbon-like ‘a‘ā and pāhoehoe lava flows (Fig. 7h), that can also be

seen on the geological maps of the volcano. Some eruption sites show branching fans, with central pāhoehoe and external ‘a‘ā zones, and an axial cone. The lava features form small, convex-upslope topographic rises that, whilst clearly visible on satellite images, are below the resolution of 90 m SRTM data. In contrast, the terrace-like structures are far wider and broader than the lava features. They occur on a sector buttressed by Hualālai to the NW, but not on rift zones of the mobile, extending SE flank that abuts Kīlauea. These features are therefore located in a zone where slope-parallel compression is possible. In view of the flexure of the island, these terraces are perhaps coupled with local sinking of the dense complex below the summit (Walker, 1992). Again, a constructional history for these structures involving superposition of many flows cannot be disregarded, but they appear to have the same general morphology and distribution as Martian flank terraces and those on Etna. The location of terraces on Mauna Loa is roughly equivalent to those on Olympus Mons, in that they are restricted to the upper flanks. Morgan and McGovern suggest that extensive gravitational spreading has occurred on both Hawaii and Olympus Mons (Morgan and McGovern, 2005). Whilst the bases of the volcanoes might have experienced outward spreading, we consider that the upper flanks may be still compressed under the relative contraction induced by flexural sinking. Such a central compressional situation was suggested by Borgia (1994) and shown to be possible by van Wyk de Vries and Matela (1998). In addition, the possible buttressing effect by Hualālai on Mauna Loa is similar to that proposed for the SE sector of Olympus Mons by the neighbouring Tharsis Rise (McGovern and Morgan, 2005). The terraces on both volcanoes are thus found in similar volcanotectonic contexts.

#### 4.5.3. Tendürek Dagi

This remote shield volcano, located in eastern Turkey, has a circular shape in plan view. Satellite images show that the volcano is built of successive, superimposing lava fields. The volcano has a fresh, little-eroded morphology, a large mass, and stands on sedimentary strata. On the SRTM slope maps we observed terrace-like structures that are arranged in a generally concentric pattern about the edifice, and have an average circumferential length of 1.5 km. Lava flow lobes are also visible in the DTM data, but have distinctive steep fronts and sides. This flow morphology is much longer and narrower than that of the terrace-like features, which, like before, do not correlate to any of the observed lava flows on imagery. Tendürek Dagi is an inaccessible volcano blighted by minefields, and thus is not easy to visit. Our remote sensing work, however, has shown the presence of terrace-like

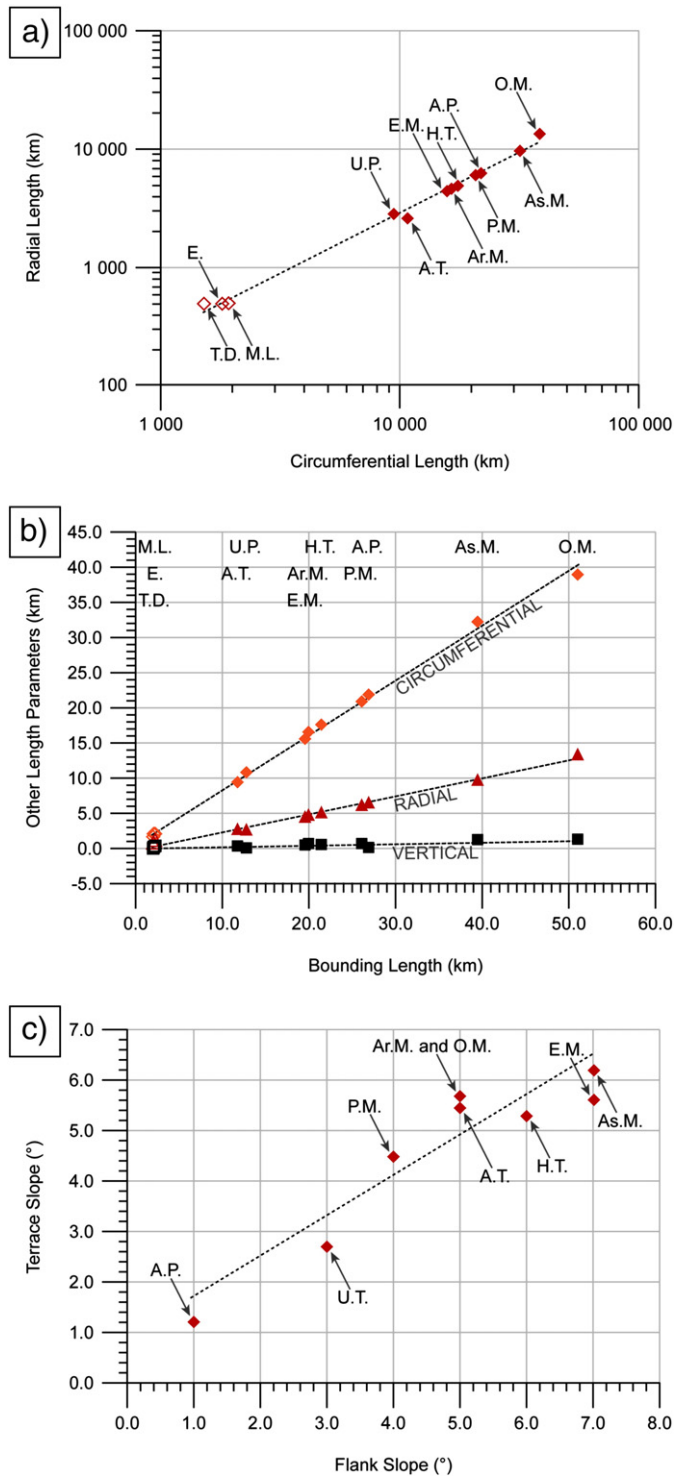


**Fig. 8.** Analysis of key terrace morphometric data. Plotted values are averages for each volcano. Individual volcanoes are identified as such: O.M. Olympus Mons; As.M. Ascaeus Mons; A.P. Alba Patera; P.M. Pavonis Mons; H.T. Hecates Tholus; Ar.M. Arsia Mons; E.M. Elysium Mons; A.T. Albor Tholus; U.P. Uranius Patera; E. Etna; M.L. Mauna Loa; and T.D. Tendürek Dagi. a.) Log–log plot of terrace circumferential length vs. radial length (after Elliot, 1976). The data are described with a power-law distribution; the trend line is of the form  $y = 0.2504x^{1.0161}$  and has an  $R^2$  value of 0.9935. b.) Linear plots of terrace circumferential and radial lengths (diamonds and triangles, respectively), and vertical height (squares), vs. terrace bounding lengths. Linear trend lines fit all data on this plot. For bounding length vs. i.) circumferential length:  $y = 0.7727x + 0.4386$ ,  $R^2 = 0.9975$ ; ii.) radial length:  $y = 0.2559x - 0.3341$ ,  $R^2 = 0.994$ ; and iii.) vertical height:  $y = 0.0244x - 0.073$ ,  $R^2 = 0.8286$ . c.) Linear plot of flank slope vs. terrace slope; the data is described by a linear trend line of the form  $y = 0.7992x + 0.8925$ , with an  $R^2$  value of 0.8448.

structures that closely correspond morphologically and spatially to those observed on the Martian volcanoes in this study.

#### 4.6. Formation mechanisms of flank terraces

Several mechanisms, both extensional and compressional, have been suggested for flank terrace formation. Each of these processes produces a characteristic set of structures (Fig. 9) whose geometry can be compared to that of flank terraces.

##### 4.6.1. Extensional mechanisms

Cipa et al. (1996) regarded terraces as concave-outward structures, bounded by outward verging normal faults accommodating volcano spreading. The interpretation of concentric dyke swarms on Arsia and Pavonis Montes led Montési (2000) to suggest that these volcanoes underwent a separate evolutionary trend to Ascaeus and Olympus Montes, which are described as terraced due to flank relaxation. Whilst concentric graben are not readily apparent on Olympus or Ascaeus Montes, MOLA data indicate that all four volcanoes are terraced, and so the mechanism of terrace formation must apply to each Tharsis Mons, and cannot be exclusive to edifices with concentric graben development. Furthermore, gravitational spreading of a volcano due to a weak substrate or underlying décollement will be apparent as an increase in basal diameter, accommodated by the development of radially orientated, concave-upward “leaf” graben (van Bemmelen, 1949; Borgia, 1994). These structures are evident on Maderas volcano, Nicaragua, which is spreading upon lacustrine and marine sediments (van Wyk de Vries and Borgia, 1996) (Fig. 9a). DTM data, however, show that Martian volcano terraces have a convex-upward, convex-outward morphology, which differs significantly from that predicted to occur due to volcano spreading.

Morgan and McGovern (2005) interpreted Olympus Mons' concave lower flanks and extensive aureole deposits as evidence for spreading of the edifice upon a central low-strength décollement (Fig. 9c). They proposed that terraces were the toes of shallow slumps mobilised during spreading, although slumping should result in subtle concave-outward head scarps, features that are not evident on this volcano or any other terraced shield. Some scarps could have been obscured by later volcanism, but there is no record of these structures even where terraces approach summit elevations on shields with a record of flank eruptions, e.g. Elysium Mons. Additionally, whilst low-competency substrata such as phyllosilicate minerals (McGovern and Morgan, 2008) may account for extensional structures at the base of Olympus Mons, its terraces are geometrically similar to those on other terraced volcanoes (Table 2, Fig. 8), most of which show no signs of distal extension at all.

##### 4.6.2. Compressional mechanisms

As Thomas et al. (1990) did not provide a mechanical definition of self-loading, we take it to mean the equilibration of a volcano's geometry under gravity, whilst the summit elevation decreases and the basal diameter remains fixed or decreases (were the base free to increase in diameter, volcano spreading would occur, accompanied by extension of the upper flanks). Thomas et al. (1990) did not consider viscoelastic stresses in their models beyond its elastic response to the applied loads, and so the behaviour of the underlying crust was not examined. Assuming then that a volcano's base does not significantly sag into the underlying crust, and that loading is restricted solely to the edifice, the volcano's volume must be conserved. Its shape will therefore evolve from conical to increasingly cylindrical. This shape change may result in the formation of radially oriented extensional structures, which are not a commonly recognised feature of large Martian shields (e.g. Crumpler and Aubele, 1978; Hodges and Moore, 1994; Plescia, 2004). Additionally, Thomas et al. (1990) suggested that a filled, high-level magma chamber within Olympus Mons, present throughout the duration of terrace formation, localised loading-

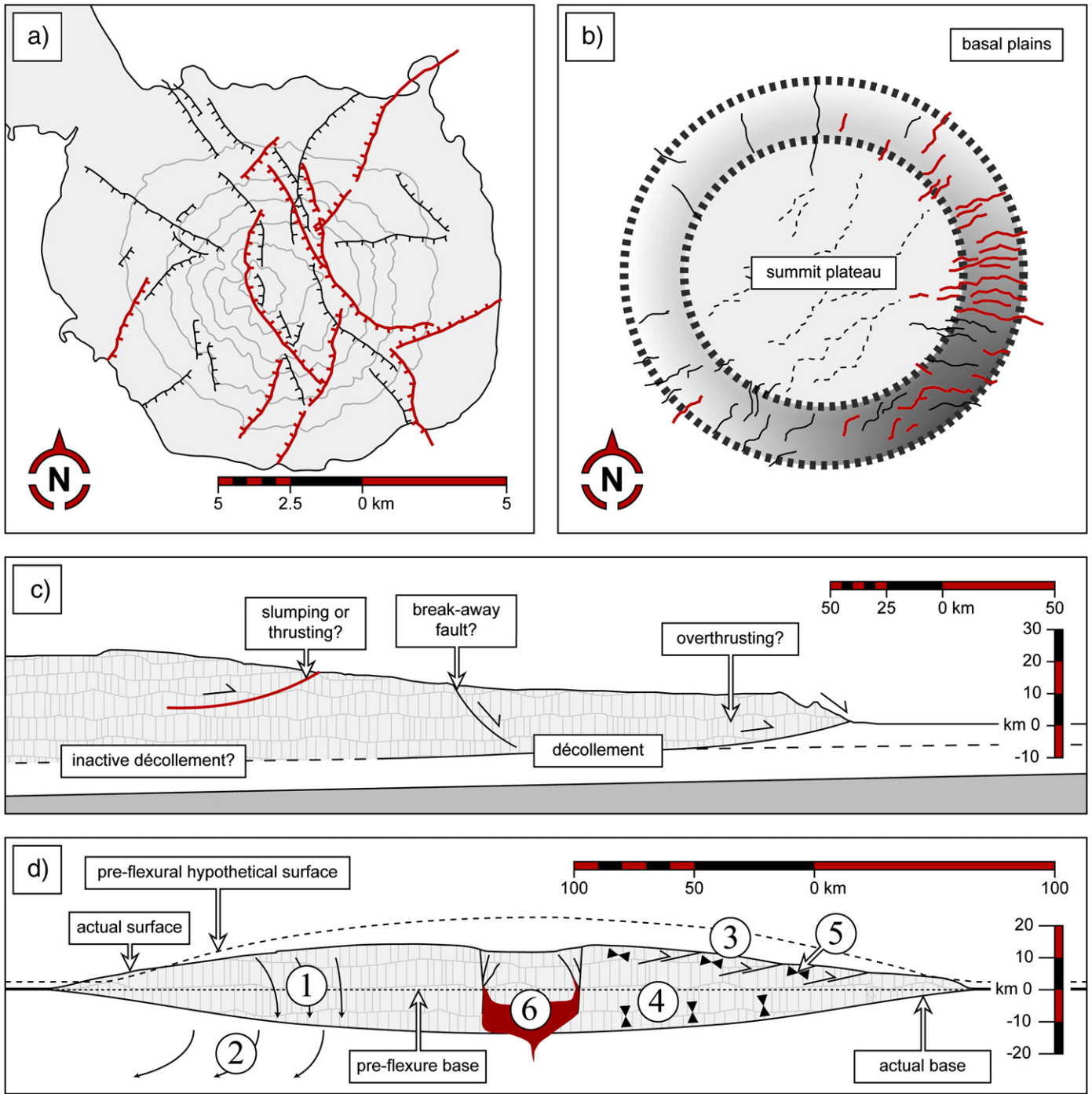


**Fig. 9.** The geometry of structures predicted by proposed terrace formation mechanisms. a.) Volcano spreading. Simplified structural map of Maderas volcano, Nicaragua, after Fig. 6 of van Wyk de Vries and Borgia (1996). Major normal faults (thick lines) cut across the edifice to form leaf graben and crescent half-graben; minor associated faults are also shown (thin lines). Ticks indicate downthrown side. Contour lines have 200 m intervals. b.) Magma chamber tumescence, after Fig. 3a of Marti et al. (1994). The predominant structure is an axisymmetric dome, the base and summit plateau of which are marked (heavy dotted lines). Sub-radial tension fractures are drawn with heavy solid lines, while smaller fractures are shown with lighter solid lines. Irregular faults that delimit the central depression are shown with a dashed stroke. Scale not given in the original figure. c.) Shallow slumping. Simplified sketch map of possible volcanotectonic structures within Olympus Mons, after Fig. 10c of Morgan and McGovern (2005). Significant structural features are shown, including a hypothesised inward-dipping fault plane (heavy line), along which thrusting may occur due to lateral flank spreading. Sketch is shown here with a 1.43× vertical exaggeration. d.) Lithospheric flexure. Stylised diagram of Ascaeus Mons undergoing lithospheric flexure. The volcano's actual surface (from a NW–SE MOLA transect) and base, and hypothesised pre-flexure surface and base, are shown. Processes at work as the volcano flexes are highlighted: (1) inward and downward displacement of volcano during flexure resulting in constriction; (2) flow or flexure of viscoelastic lithosphere; (3) near-surface thrusts and undulations forming flank terraces; (4)  $\sigma_1$  – vertical due to load; (5)  $\sigma_1$  low-angle due to constriction. The magma chamber is also shown (6). Sketch is shown with no vertical exaggeration.

induced compressive stresses at elevations that agree with their observed positions of terraces high upon the volcano's flanks. DTM data show that terraces are not restricted to the upper flank of Olympus, however, nor are they localised so on any other terraced edifice.

Marti et al. (1994) showed that magma chamber growth results in the formation of a dome above the chamber, accommodated by inward-dipping concentric reverse faults. Crumpler et al. (1996) suggested that the cumulative effects of such chamber tumescence could result in the steepening of volcano flanks, and possibly in the

formation of terraces. Terrace morphology does not support this hypothesis, however. Whilst the concentric faults of [Marti et al. \(1994\)](#) bounded a convex-upward structure, they did not form an intersecting “fish scale” pattern like those of terrace bounding faults. Therefore, the domical structure so formed did not resemble flank terraces ([Fig. 9b](#)). Additionally, with continued inflation the dome's upper surface developed a polygonal network of fractures, evidence for which is lacking on the upper flanks of terraced Martian shields. These polygonal fracture patterns, coupled with radial fractures, also developed in experiments conducted by [Walter and Troll \(2001\)](#) and [Troll et al. \(2002\)](#), who modelled chamber tumescence beneath both a flat surface and cones of varying geometries. [Marti et al. \(1994\)](#) and [Walter and Troll \(2001\)](#) concluded that upon evacuation of the magma chamber these faults could invert their sense of throw, becoming normal ring faults. This activity could potentially serve to offset the effects of cumulative magma chamber tumescence and any associated structures. The compressional stresses associated with magma chamber inflation manifest circumferentially about the chamber ([Marti et al., 1994](#)), yet several of the terraced Martian shields bear no evidence of terracing on certain sectors, e.g. to the SW of Hecates Tholus, and on the E flank of Uranus Patera. This may be due to the localisation of stresses within these volcanoes (see Section 4.3.2). Conversely, these perceived preferential zones of terracing may be due to other factors (see Section 4.4). In addition, whilst tumescence produces uplift above an inflating chamber, terraces occur at flank elevations close to or at the base of the cone on several volcanoes, e.g. Ascræus Mons and Hecates Tholus ([Table 2](#)). These structures are thus below any shallow magma chamber responsible for caldera formation, assuming shallow chambers are located at neutral buoyancy zones within the edifice (e.g. [Zuber and Mouginis-Mark, 1992](#); [Wilson and Head, 1994](#)).

A large volcanic load can induce flexure of the underlying lithosphere, and can in turn affect the stress fields within the edifice. The presence of circumferential graben and flexural troughs about some of the largest Martian shields indicates that lithospheric flexure has indeed occurred ([Comer et al., 1985](#); [Zuber et al., 1993](#)). Flexure may produce wholly compressive structures that match terrace geometry well, in response to the horizontal compression of an edifice. The development of a flexural depression beneath a volcano might serve to reduce its elevation, whilst a proximal flexural bulge may prevent the basal diameter from increasing, and could even reduce it. The volcano enters a state of stress where  $\sigma_1$  is radial,  $\sigma_2$  concentric, and  $\sigma_3$  vertical ([van Wyk de Vries and Matela, 1998](#)). Strain is apparent in this case as a net reduction in surface area, accommodated by outward verging circumferential thrusts ([McGovern and Solomon, 1993](#)). We consider these structures to correspond to flank terraces ([Fig. 9d](#)). As the entire edifice is likely to experience the effects of flexure, these structures may form across a wide range of elevations, similar to what is observed on Mars and Earth.

Furthermore, whilst certain extensional structures do exist on the flanks of several large Martian shields ([Hodges and Moore, 1994](#)), flexure does not require the formation of radially oriented tension fractures, structures that are predicted by other formation mechanism hypotheses but are conspicuously absent on terraced volcanoes. [McGovern and Solomon \(1993\)](#) modelled instantaneous and incremental emplacement of volcanic loads welded to an elastic lithosphere, and found that both situations generated circumferentially oriented thrusts. Latter-stage units emplaced incrementally in their models did not experience compressional failure. Terraces are visible today, however, long after the volcano construction phase has presumably finished. This suggests that terraces are not in fact produced during the emplacement of discrete lava flows, as horizontal compressive stresses decrease with each successive load increment ([McGovern and Solomon, 1993](#)). Additionally, later volcanism could completely obscure earlier terrace traces, were they to be formed. Instead, terracing must occur, at least in some cases, after most

volcanism has taken place and can thus be a late-stage event. This scenario may be similar to [McGovern's and Solomon's](#) model of an instantaneously emplacement load, where formation of a volcano is rapid relative to the time required for the lithosphere to flex. A short main shield-building phase for Martian volcanoes is possible, if eruption/effusion rates were sufficiently high (e.g. [Plescia, 2000](#)).

#### 4.6.3. Applicability to Mars and Earth

Elastic self-loading, whilst likely to occur in large volcanoes on Mars and Earth, does not adequately account for the morphology and distribution of flank terraces. Additionally, [Thomas et al. \(1990\)](#) invoke a specific magma chamber condition for Olympus Mons to account for their perceived distribution of terraces that may not be applicable for other terraced edifices on either planet. Magma chamber tumescence does not generate convexities matching the “fish scale” terrace-stacking pattern, but does produce radial fractures that we do not observe; additionally, this mechanism cannot account for the elevations and distributions of terraces upon many of the studied shields. Volcano spreading and gravitational slumping produce negative-relief flank structures that do not match the characteristic convex-upward terrace profile. Neither slump scarps nor radial graben are spatially coincident with flank terraces on any of the Martian or Terran volcanoes we observed. However, lithospheric flexure can produce structures that, as surface expressions of shallow faults formed as a volcano's surface area decreases, match the compressional geometry of flank terraces. Flexure could also account for the development of terraces late in an edifice's active lifetime. This process may be common to all volcanoes discussed herein by virtue of their large masses inducing flexure. Indeed, there is evidence that flexure has occurred underneath many of the large volcanoes on Mars and Earth. If terraces develop in response to a net reduction in volcano surface area, however, flexure may not be the only mechanism capable of generating these structures. Regional tectonism (e.g. across Etna) or topographic buttressing (e.g. on the SE flanks of Olympus Mons and Mauna Loa) may also serve to constrict the upper surface of a volcano as effectively as lithospheric flexure, thus leading to the formation of flank terraces too.

## 5. Concluding remarks

We have presented a comprehensive description of flank terrace morphology and distribution. Terraces occur on at least nine Martian and three Terran shield volcanoes. The convex-upward, convex-outward terrace morphology resembles that of thrust faults on Earth, whilst the ubiquitous, imbricate “fish scale” terrace stacking pattern suggests a systematic process of formation for these structures. Morphometric data indicates that terraces are scale-invariant structures. Their presence on volcanoes that differ in size, age, and location across Mars and Earth implies that they are a fundamental volcanotectonic structure. By comparing our observations of terrace geometry with those predicted by existing formation hypotheses, we conclude that lithospheric flexure is the primary agent responsible for flank terrace formation. More work is required to provide a complete account of the role terraces play within the volcanotectonic evolution of large shield volcanoes. Nonetheless, we propose that flank terraces are the surface expressions of thrust faults, that they occur on Mars and Earth, and that terraced volcanoes on both planets should be viewed within a paradigm of lithospheric flexure.

## Acknowledgements

This work has been supported by a Postgraduate Research Studentship from Trinity College Dublin for PKB, and the Enterprise Ireland International Collaboration programme (grant no. IC/2006/37/1138) for PKB and VRT. The thesis of PKB is a Cotutelle between Trinity College Dublin and Université Blaise-Pascal. We thank E.

Holohan for his insightful and constructive comments, and M. Balme for his GIS mentoring. J. Byrne, P. Dunne, and B. Durcan are thanked for their terrace mapping efforts. The comments of John Walsh of the Fault Analysis Group, University College Dublin, and two anonymous reviewers greatly improved the quality of this manuscript, and are much appreciated. This research has made use of NASA's Planetary Data System and Astrophysics Data System.

## Appendix A. Supplementary data

Supplementary data associated with this article can be found, in the online version, at doi:10.1016/j.epsl.2009.01.043.

## References

- Bleacher, J.E., Greeley, R., Williams, D.A., Cave, S.R., Neukum, G., 2007. Trends in effusive style at the Tharsis Montes, Mars, and implications for the development of the Tharsis province. *J. Geophys. Res.* 112. doi:10.1029/2006JE002873.
- Borgia, A., 1994. Dynamic basis of volcanic spreading. *J. Geophys. Res.* 99, 17791–17804.
- Borgia, A., Ferrari, L., Pasquarè, G., 1992. Importance of gravitational spreading in the tectonic and volcanic evolution of Mount Etna. *Nature* 357, 231–235.
- Borgia, A., van Wyk de Vries, B., 2003. The volcano-tectonic evolution of Concepción, Nicaragua. *Bull. Volcanol.* 65, 248–266.
- Branquet, Y., van Wyk de Vries, B., 2001. Effects of volcanic loading on regional compressive structures: new insights from natural examples and analogue modelling. *C. R. Acad. Sci., Sér. IIA* 333, 455–461.
- Byrne, P.K., Murray, J.B., van Wyk de Vries, B., Troll, V.R., 2007. Flank terrace architecture of Martian shield volcanoes. 38th Lunar and Planetary Science Conference, Abstract 2380.
- Carr, M.H., Greeley, R., Blasius, K.R., Guest, J.E., Murray, J.B., 1977. Some Martian volcanic features as viewed from the Viking orbiters. *J. Geophys. Res.* 82, 3985–4015.
- Chester, D.K., Duncan, A.M., Guest, J.E., Kilburn, C., 1985. Mount Etna: Anatomy of a Volcano. Chapman and Hall Ltd., London, p. 300.
- Cipa, A., Bébien, J., Bonin, B., 1996. Les terrasses et l'escarpement basal du volcan Martien Olympus Mons: Des témoins de vastes glissements gravitaires des flancs? *C. R. Acad. Sci., Sér. II* 322, 369–376.
- Comer, R.P., Solomon, S.C., Head, J.W., 1985. Mars: thickness of the lithosphere from the tectonic response to volcanic loads. *Rev. Geophys.* 23, 61–92.
- Crown, D.A., Greeley, R., 1993. Volcanic geology of Hadriaca Patera and the eastern Hellas region of Mars. *J. Geophys. Res.* 98, 3431–3451.
- Crumpler, L.S., Aubele, J.C., 1978. Structural evolution of Arsia Mons, Pavonis Mons and Ascræus Mons: Tharsis region of Mars. *Icarus* 34, 496–511.
- Crumpler, L.S., Head, J.W., Aubele, J.C., 1996. Calderas on Mars: characteristics, structure and associated flank deformation. In: McGuire, W.J., Jones, A.P., Neuberger, J. (Eds.), *Volcano Instability on the Earth and Other Planets*. *Geol. Soc. Spec. Pap.*, vol. 110, pp. 307–348.
- Elliott, D., 1976. The energy balance and deformation mechanisms of thrust sheets. *Phil. Trans. R. Soc. Lond.* 283, 289–312.
- Farr, T.G., Rosen, P.A., Caro, E., Crippen, R., Duren, R., Hensley, S., Kobrick, M., Paller, M., Rodriguez, E., Roth, L., Seal, D., Shaffer, S., Shimada, J., Umland, J., Werner, M., Oskin, M., Burbank, D., Alsdorf, D., 2007. The shuttle radar topography mission. *Rev. Geophys.* 45. doi:10.1029/2005RC00183.
- Head, J.W., Solomon, S.C., 1981. Tectonic evolution of the terrestrial planets. *Science* 213, 62–76.
- Hodges, C.A., Moore, H.J., 1994. Atlas of volcanic landforms on Mars. U.S. Geological Survey Professional Paper, vol. 1534. United States Government Printing Office, Washington, p. 194.
- Krall, E.R., van Dijk, M., Postmal, G., Kleinhaus, M.G., 2008. Martian stepped-delta formation by rapid water release. *Nature* 451, 973–976.
- Marti, J., Ablay, G.J., Redshaw, L.T., Sparks, R.S.J., 1994. Experimental studies of collapse calderas. *J. Geophys. Res.* 99, 919–929.
- McGovern, P.J., Morgan, J.K., 2005. Spreading of the Olympus Mons volcanic edifice. Mars. 36th Lunar and Planetary Science Conference, Abstract 2258.
- McGovern, P.J., Solomon, S.C., 1993. State of stress, faulting, and eruption characteristics of large volcanoes on Mars. *J. Geophys. Res.* 98, 23553–23579.
- McGovern, P.J., Morgan, J.K., 2008. Volcanic spreading at Olympus Mons: new models, with implications for Martian volcanic edifice structures and the distribution of phyllosian sediments. Lunar and Planetary Science Conference, Abstract 2304.
- Montési, L.G.J., 1999. Concentric dike swarm and internal structure of Pavonis Mons (Mars). 30th Lunar and Planetary Science Conference, Abstract 1251.
- Montési, L.G.J., 2000. Concentric dike swarms on the flanks of Pavonis Mons: implications for the evolution of Martian shield volcanoes and mantle plumes. In: Ernst, R.E., Buchan, K.L. (Eds.), *Locating Pre-Mesozoic Mantle Plumes*. *Geol. Soc. Spec. Pap.*, vol. 352, pp. 165–181.
- Morgan, J.K., McGovern, P.J., 2005. Discrete element simulations of gravitational volcanic deformation: 1. Deformation structures and geometries. *J. Geophys. Res.* 110. doi:10.1029/2004JB003252.
- Morris, E.C., 1981. Structure of Olympus Mons and its basal scarp. Third International Colloquium on Mars, LPI Contribution 441 (1981LPICo.441.161M).
- Mouginis-Mark, P.J., Wilson, L., Head, J.W., Brown, S.H., Hall, J.L., Sullivan, K.D., 1984. Elysium Planitia, Mars: regional geology, volcanology, and evidence for volcano-ground ice interactions. *Earth Moon Planet.* 30, 149–173.
- Neukum, G., Jaumann, R., Hoffmann, H., Hauber, E., Head, J.W., Basilevsky, A.T., Ivanov, B.A., Werner, S.C., van Gasselt, S., Murray, J.B., McCord, T., The HRSC Co-Investigator Team, 2004. Recent and episodic volcanic and glacial activity on Mars revealed by the High Resolution Stereo Camera. *Nature* 432, 971–979.
- Plescia, J.B., 2000. Geology of the Uranius group volcanic constructs: Uranius Patera, Ceraunius Tholus, and Uranius Tholus. *Icarus* 143, 376–396.
- Plescia, J.B., 2004. Morphometric properties of Martian volcanoes. *J. Geophys. Res.* 109. doi:10.1029/2002JE002031.
- Plescia, J.B., 2007. Volcanology of the Elysium volcanoes. 38th Lunar and Planetary Science Conference, Abstract 2141.
- Roche, O., van Wyk de Vries, B., Druitt, T.H., 2001. Sub-surface structures and collapse mechanisms of summit pit craters. *J. Vol. Geotherm. Res.* 105, 1–18.
- Smith, D.E., Zuber, M.T., Frey, H.V., Garvin, J.B., Head, J.W., Muhleman, D.O., Pettengill, G.H., Phillips, R.J., Solomon, S.C., Zwally, H.J., Banerdt, W.B., Duxbury, T.C., Golombek, M.P., Lemoine, F.G., Neumann, G.A., Rowlands, D.D., Aharonson, O., Ford, P.G., Ivanov, A.B., Johnson, C.L., McGovern, P.J., Abshire, J.B., Afzal, R.S., Sun, X., 2001. Mars Orbiter Laser Altimeter: experiment summary after the first year of global mapping of Mars. *J. Geophys. Res.* 106, 23689–23722.
- Thomas, P.J., Squyres, S.W., Carr, M.H., 1990. Flank tectonics of Martian volcanoes. *J. Geophys. Res.* 95, 14345–14355.
- Troll, V.R., Walter, T.R., Schmincke, H.-U., 2002. Cyclic caldera collapse: piston or piecemeal subsidence? Field and experimental evidence. *Geology* 30, 135–138.
- Twiss, R.J., Moores, E.M., 1992. *Structural Geology*. W. H. Freeman & Co., New York, p. 532.
- van Bemmelen, R.W., 1949. *The Geology of Indonesia*. General Geology of Indonesia and Adjacent Archipelagos. Government Printing Office, The Hague. 1A.
- van Wyk de Vries, B., Borgia, A., 1996. The role of basement in volcano deformation. In: McGuire, W.J., Jones, A.P., Neuberger, J. (Eds.), *Volcano Instability on the Earth and Other Planets*. *Geol. Soc. Spec. Pap.*, vol. 110, pp. 95–110.
- van Wyk de Vries, B., Matela, R., 1998. Styles of volcano-induced deformation: numerical models of substratum flexure, spreading and extrusion. *J. Vol. Geotherm. Res.* 81, 1–18.
- Walker, G.P.L., 1992. “Coherent intrusion complexes” in large basaltic volcanoes – a new structural model. *J. Vol. Geotherm. Res.* 50, 41–54.
- Walter, T.R., Troll, V.R., 2001. Formation of caldera periphery faults: an experimental study. *Bull. Vol.* 63, 191–203.
- Walsh, J.J., Watterson, J., 1991. Geometric and kinematic coherence and scale effects in normal fault systems. *Geol. Soc. Lond. Spec. Pub.* 56, 193–203.
- Wilson, L., Head, J.W., 1994. Mars: review and analysis of volcanic eruptions theory and relationships to observed landforms. *Rev. Geophys.* 32, 221–263.
- Zimbleman, J.R., Edgett, K.S., 1992. The Tharsis Montes, Mars: comparison of volcanic and modified landforms. *Proc. Lunar Planet. Sci.* 22, 31–44.
- Zuber, M.T., Mouginis-Mark, P.J., 1992. Caldera subsidence and magma chamber depth of the Olympus Mons volcano, Mars. *J. Geophys. Res.* 97, 18295–18307.
- Zuber, M.T., Smith, D.E., Solomon, S.C., Muhleman, D.O., Head, J.W., Garvin, J.B., Abshire, J.B., Bufton, J.L., 1992. The Mars Observer laser altimeter investigation. *J. Geophys. Res.* 97, 7781–7797.
- Zuber, M.T., Bills, B.G., Frey, H.V., Kiefer, W.S., Nerem, R.S., Roark, J.H., 1993. Possible flexural signatures around Olympus and Ascræus Montes, Mars. 24th Lunar and Planetary Science Conference, Abstract 1591.